< Electronic Supporting Information>

Modulated assembly and structural diversity of heterometallic Sn-Ti oxo clusters from inorganic tin precursors

Hui-Fang Zhao,[a] Fang-Fang Liu,[a] Qing-Rong Ding,[a] Di Wang,[a] Jian Zhang,[a] and Lei Zhang[a,b*]

[a]*State Key Laboratory of Structural Chemistry, Fujian Institute of Research on the Structure of Matter, Chinese Academy of Sciences, Fuzhou, Fujian 350002, China.*
[b]*Institute of Modern Optics, College of Electronic Information and Optical Engineering, Nankai University, Tianjin 300350, China.*
E-mail: zhanglei3915@nankai.edu.cn.

Content

1. Materials and instruments

All the reagents and solvents employed are purchased commercially and used as received without further treatment. $SnCl_2·2H_2O$ and $SnCl_4·5H_2O$ were purchased from Energy Chemical, trimethylolpropane and di(trimethylolpropane) were purchased from Aladdin. $Ti(O^iPr)_4$ was purchased from Adamas, while ethyl acetate, acetonitrile, 1,4-dioxane, formic acid, acetic acid and propionic acid were bought from Sino pharm Chemical Reagent Beijing. Powder X-ray diffraction (PXRD) analyses data were mounted on a Rigaku Mini Flex II diffractometer using Cu Kα radiation (λ = 1.54056 Å) under ambient conditions. Fourier transform infrared (FT-IR) spectra were recorded with a Spectrum One FT-IR Spectrometer in the 400-4000 cm^{-1} range. Thermal stabilities were investigated by a Mettler Toledo TGA/SDTA 851e analyzer in N_2 atmosphere with a heating rate of 10 ℃/min under N_2 atmosphere. Elemental analyses were measured on a Vario MICRO Elemental Analyzer instrument. The UV−vis diffuse reflection data were recorded at room temperature using a powder sample with $BaSO_4$ as a standard (100% reflectance) on a PerkinElmer Lamda-950 UV spectrophotometer and scanned from 200 to 800 nm. The energy dispersive spectroscopy (EDS) analyses of single crystals were performed on a JEOL JSM6700F field-emission scanning electron microscope equipped with an Oxford INCA system. ESI-MS was carried out on Thermo Scientific Exactive Plus. Inductively coupled plasma (ICP) analyses for Sn and Ti were conducted on an Ultima2 spectrometer. X-ray photoelectron spectroscopy (XPS) analysis was carried out on ESCALAB Xi^+ XPS system (Thermo Fisher Scientific) with Al Kα X-ray radiation (1486.6 eV). Routine ^1H NMR spectra were recorded on a Bruker AVANCE III (400 MHz for ^1H NMR). Gas chromatography (GC) was performed with an GC-2014C (SHIMADZU) gas chromatography system equipped with flame ionization detectors and a thermal conductivity detector (TCD). The liquid products were detected by CIC-D100 automatic range ion chromatograph.

2. Synthesis

Synthesis of TOC-51

$SnCl_4·5H_2O$ (0.35 g, 1.0 mmol), trimethylolpropane (0.27 g, 2.0 mmol), 1,4-dioxane (4 ml) and 4 ml ethyl acetate were mixed together. Then $Ti(O^iPr)_4$ (0.50 ml, 1.50 mmol) was added. The mixture were mixed and sealed in a 20 mL vial, and then transferred to a preheated oven at 80 °C and heated for 3 days. After Leave the vial at room temperature for 6 days, colorless crystals of **TOC-51** were obtained with a yield of ~45% based on Sn. Elemental analysis (%): Calcd for $C_{72}H_{142}Cl_{18}O_{50}Sn_6Ti_{10}$: C, 23.78; H, 3.94. Found: C, 23.8; H, 4.01.

Synthesis of TOC-52

$SnCl_4·5H_2O$ (0.35g, 1.0 mmol), trimethylolpropane (0.27 g, 2.0 mmol), 1,4-dioxane (6 ml) and 1 ml propionic acid were mixed together. Then $Ti(O^iPr)_4$ (0.50 ml, 1.50 mmol) was added. The mixture were mixed and sealed in a 20 mL vial, and then transferred to a preheated oven at 80 °C and heated for 3 days. After Leave the vial at room temperature for 6 days, colorless crystals of **TOC-52** were obtained with a yield of ~33% based on Sn. Elemental analysis (%): Calcd for $C_{74}H_{146}Cl_{18}O_{50}Sn_6Ti_{10}$: C, 24.25; H, 4.02. Found: C, 24.73; H, 4.03.

Synthesis of TOC-53

$SnCl_4 \cdot 5H_2O$ (0.35 g, 1.0 mmol), di(trimethylolpropane) (0.25 g, 1.0 mmol), acetonitrile (2 ml) and 4 ml ethyl acetate were mixed together. Then $Ti(O^iPr)_4$ (0.50 ml, 1.50 mmol) was added. The mixture were mixed and sealed in a 20 mL vial, and then transferred to a preheated oven at 80 °C and heated for 5 days. After cooling to room temperature, colorless crystals of **TOC-53** were obtained with a yield of ~27% based on Sn. Elemental analysis (%): Calcd for $C_{14}H_{25}Cl_3O_7SnTi$: C, 29.08; H, 4.36. Found: C, 29.17; H, 4.36.

Synthesis of TOC-54

$SnCl_4 \cdot 5H_2O$ (0.35 g, 1.0 mmol), di(trimethylolpropane) (0.25 g, 1.0 mmol), acetonitrile (5 ml) and 2 ml propionic acid were mixed together. Then $Ti(O^iPr)_4$ (0.50 ml, 1.50 mmol) was added. The mixture were mixed and sealed in a 20 mL vial, and then transferred to a preheated oven at 80 °C and heated for 5 days. After cooling to room temperature, colorless crystals of **TOC-54** were obtained with a yield of ~37% based on Sn. Elemental analysis (%): Calcd for $C_{15}H_{27}Cl_3O_7SnTi$: C, 30.42; H, 4.59. Found: C, 27.36; H, 4.34.

Synthesis of TOC-55

$SnCl_4 \cdot 5H_2O$ (0.35 g, 1.0 mmol), di(trimethylolpropane) (0.25 g, 1.0 mmol), acetonitrile (3 ml) and 3 ml 1,4-dioxane were mixed together. Then $Ti(O^iPr)_4$ (0.50 ml, 1.50 mmol) was added. The mixture were mixed and sealed in a 20 mL vial, and then transferred to a preheated oven at 80 °C and heated for 5 days. After cooling to room temperature, colorless crystals of **TOC-55** were obtained with a yield of ~36% based on Sn. Elemental analysis (%): Calcd for $C_{24}H_{48}Cl_6O_{13}Sn_2Ti_2$: C, 26.43; H, 4.44. Found: C, 30.08; H, 5.10.

Synthesis of TOC-56

$SnCl_4 \cdot 5H_2O$ (0.35 g, 1.0 mmol), di(trimethylolpropane) (0.25 g, 1.0 mmol), acetonitrile (5 ml) and 50 μL propionic acid were mixed together. Then $Ti(O^iPr)_4$ (0.50 ml, 1.50 mmol) was added. The mixture were mixed and sealed in a 20 mL vial, and then transferred to a preheated oven at 80 °C and heated for 5 days. After cooling to room temperature, colorless crystals of **TOC-56** were obtained with a yield of ~65% based on Sn. Elemental analysis (%): Calcd for $C_{48}H_{90}Cl_6O_{26}Sn_2Ti_6$: C, 31.67; H, 4.98. Found: C, 28.69; H 4.93.

Synthesis of TOC-57

$SnCl_2 \cdot 2H_2O$ (0.34 g, 1.5 mmol), di(trimethylolpropane) (0.25g, 1.0 mmol), acetonitrile (5 ml) and 50 μL acetic acid were mixed together. Then $Ti(O^iPr)_4$ (0.50 ml, 1.50 mmol) was added. The mixture were mixed and sealed in a 20 mL vial, and then transferred to a preheated oven at 80 °C and heated for 5 days. After cooling to room temperature, yellow crystals of **TOC-57** were obtained with a yield of ~88% based on Sn. Elemental analysis (%): Calcd for $C_{96}H_{178}Cl_{14}O_{54}Sn_6Ti_{14}$: C, 28.29; H, 4.40. Found: C, 28.47; H, 4.52.

Synthesis of TOC-58

$SnCl_2 \cdot 2H_2O$ (0.34 g, 1.5 mmol), di(trimethylolpropane) (0.25 g, 1.0 mmol), acetonitrile (5 ml) and 50 μL formic acid were mixed together. Then $Ti(O^iPr)_4$ (0.50 ml, 1.50 mmol) was added. The mixture were mixed and sealed in a 20 mL vial, and then transferred to a preheated oven at 80 °C and heated for 5 days. After cooling to room temperature, red crystals of **TOC-58** were

obtained with a yield of ~35% based on Sn. Elemental analysis (%): Calcd for $C_{144}H_{264}Cl_{12}O_{82}Sn_8Ti_{20}$: C, 30.67; H, 4.72. Found: C, 27.18; H, 4.62.

3. Single-crystal X-ray diffraction

Single-crystal diffraction data for compounds were collected on Hybrid Pixel Array detector equipped with Ga-Kα radiation (λ= 1.3405 Å). Using Olex2,[1] the structures were solved with the dual-direct methods using ShelxT and refined with the full-matrix least-squares technique based on F^2 using the *SHELXL*.[2-4] Non-hydrogen atoms were refined anisotropically. Hydrogen atoms were added theoretically. The obtained crystallographic data for compound summarized in Table S1–S4. The X-ray crystallographic coordinates for structures reported in this article have been deposited at the Cambridge Crystallographic Data Centre (CCDC) under deposition numbers CCDC 2365528-2365535. These data can be obtained free of charge from the Cambridge Crystallographic Data Centre via http://www.ccdc.cam.ac.uk/data_request/cif.

Table S1 Crystal data and structure refinement for **TOC-51** and **TOC-52**.

Compound	**TOC-51**	**TOC-52**
Crystal formula	$C_{72}H_{142}Cl_{18}O_{50}Sn_6Ti_{10}$	$C_{74}H_{146}Cl_{18}O_{50}Sn_6Ti_{10}$
Formula weight	3636.95	3665.14
Temperature/K	100.0(3)	293(2)
Crystal system	triclinic	monoclinic
Space group	*P*-1	*P*21/*n*
a/Å	12.9762(2)	15.60310(10)
b/Å	22.6922(3)	18.1016(2)
c/Å	26.2336(3)	29.8915(2)
α/°	111.5130(10)	90
β/°	96.0020(10)	96.5800(10)
γ/°	96.3570(10)	90
Volume/Å^3	7053.79(17)	8386.97(12)
Z	2	2
ρ_{calc}g/cm^3	1.712	1.451
μ/mm^{-1}	11.260	9.473
F(000)	3598.0	3632.0
Radiation	micro-focus metaljet (λ = 1.3405)	micro-focus metaljet (λ = 1.3405)
2Θ range for data collection/°	3.686 to 120.854	4.97 to 120.286
Index ranges	-15 ≤ h ≤ 16, -29 ≤ k ≤ 27, -33 ≤ l ≤ 33	-20 ≤ h ≤ 19, -22 ≤ k ≤ 22, -31 ≤ l ≤ 38
Reflections collected	101285	75852
Independent reflections	31498 [R_{int} = 0.0480, R_{sigma} = 0.0460]	18686 [R_{int} = 0.0619, R_{sigma} = 0.0508]
Data/restraints/parameters	31498/4/1420	18686/0/738
Goodness-of-fit on F^2	1.049	1.033
Final R indexes [I>=2σ (I)]	R_1 = 0.0437, $_wR_2$ = 0.1063	R_1 = 0.0584, $_wR_2$ = 0.1690

Final R indexes [all data]	R_1 = 0.0515, $_wR_2$ = 0.1109	R_1 = 0.0660, $_wR_2$ = 0.1766
Largest diff. peak/hole / e Å^{-3}	3.48/-2.28	3.80/-1.92

Table S2 Crystal data and structure refinement for **TOC-53** and **TOC-54**.

Compound	**TOC-53**	**TOC-54**
Crystal formula	$C_{14}H_{25}Cl_3O_7SnTi$	$C_{15}H_{27}Cl_3O_7SnTi$
Formula weight	578.28	592.30
Temperature/K	100.00(10)	100.00(10)
Crystal system	monoclinic	triclinic
Space group	$P2_1/c$	P-1
a/Å	9.85680(10)	9.0964(2)
b/Å	16.8341(3)	9.3132(2)
c/Å	12.5136(2)	14.5943(3)
α/°	90	73.634(2)
β/°	92.6740(10)	89.391(2)
γ/°	90	67.044(2)
Volume/Å^3	2074.13(5)	1085.42(4)
Z	4	2
ρ_{calc}g/cm^3	1.852	1.812
μ/mm^{-1}	11.341	10.846
F(000)	1152.0	592.0
Radiation	micro-focus metaljet (λ = 1.3405)	micro-focus metaljet (λ = 1.3405)
2Θ range for data collection/°	7.658 to 120.342	5.522 to 119.932
Index ranges	-12 ≤ h ≤ 12, -21 ≤ k ≤ 20, -8 ≤ l ≤ 16	-11 ≤ h ≤ 10, -12 ≤ k ≤ 11, -18 ≤ l ≤ 18
Reflections collected	17404	13333
Independent reflections	4619 [R_{int} = 0.0490, R_{sigma} = 0.0417]	4791 [R_{int} = 0.0310, R_{sigma} = 0.0286]
Data/restraints/parameters	4619/0/238	4791/0/247
Goodness-of-fit on F^2	1.077	1.043
Final R indexes [I>=2σ (I)]	R_1 = 0.0377, $_wR_2$ = 0.1028	R_1 = 0.0241, $_wR_2$ = 0.0612
Final R indexes [all data]	R_1 = 0.0416, $_wR_2$ = 0.1051	R_1 = 0.0247, $_wR_2$ = 0.0616
Largest diff. peak/hole / e Å^{-3}	1.36/-1.56	0.92/-0.90

Table S3 Crystal data and structure refinement for **TOC-55** and **TOC-56**.

Compound	**TOC-55**	**TOC-56**
Crystal formula	$C_{24}H_{48}Cl_6O_{13}Sn_2Ti_2$	$C_{48}H_{88}Cl_6O_{26}Sn_2Ti_6$
Formula weight	1090.50	1820.55
Temperature/K	100.00(10)	100.0(2)
Crystal system	monoclinic	triclinic
Space group	*Cc*	*P*-1
a/Å	8.98520(10)	12.3168(4)

b/Å	18.3443(2)	14.0058(4)
c/Å	25.5115(2)	15.4344(3)
α/°	90	110.064(2)
β/°	95.5520(10)	92.418(2)
γ/°	90	112.772(3)
Volume/Å^3	4185.26(7)	2258.45(12)
Z	4	1
ρ_{calc}g/cm^3	1.731	1.337
μ/mm^{-1}	11.200	7.285
F(000)	2168.0	918.0
Radiation	micro-focus metaljet (λ = 1.3405)	micro-focus metaljet (λ = 1.3405)
2Θ range for data collection/°	6.052 to 120.164	6.462 to 120.328
Index ranges	-5 ≤ h ≤ 11, -22 ≤ k ≤ 23, -32 ≤ l ≤ 32	-15 ≤ h ≤ 15, -18 ≤ k ≤ 16, -19 ≤ l ≤ 19
Reflections collected	15569	27705
Independent reflections	5471 [R_{int} = 0.0320, R_{sigma} = 0.0323]	9981 [R_{int} = 0.0727, R_{sigma} = 0.0659]
Data/restraints/parameters	5471/2/430	9981/1/401
Goodness-of-fit on F^2	1.048	1.077
Final R indexes [I>=2σ (I)]	R_1 = 0.0333, $_wR_2$ = 0.0890	R_1 = 0.0620, $_wR_2$ = 0.1759
Final R indexes [all data]	R_1 = 0.0337, $_wR_2$ = 0.0894	R_1 = 0.0687, $_wR_2$ = 0.1815
Largest diff. peak/hole / e Å^{-3}	1.17/-0.77	2.89/-1.90

Table S4 Crystal data and structure refinement for **TOC-57** and **TOC-58**.

Compound	**TOC-57**	**TOC-58**
Crystal formula	$C_{96}H_{178}Cl_{14}O_{54}Sn_6Ti_{14}$	$C_{144}H_{264}Cl_{12}O_{82}Sn_8Ti_{20}$
Formula weight	4075.41	5640.46
Temperature/K	100.00(13)	100.00(17)
Crystal system	monoclinic	cubic
Space group	*P*2$_1$/*c*	*I*-43*d*
a/Å	15.2738(2)	41.7993(2)
b/Å	23.1167(2)	41.7993(2)
c/Å	23.1453(2)	41.7993(2)
α/°	90	90
β/°	106.9090(10)	90
γ/°	90	90
Volume/Å^3	7818.84(15)	73031.0(10)
Z	2	12
ρ_{calc}g/cm^3	1.731	1.539
μ/mm^{-1}	10.899	9.164
F(000)	4064.0	33936.0
Radiation	micro-focus metaljet (λ = 1.3405)	micro-focus metaljet (λ = 1.3405)

2Θ range for data collection/°	4.804 to 120.398	4.502 to 120.446
Index ranges	-18 ≤ h ≤ 19, -29 ≤ k ≤ 28, -29 ≤ l ≤ 24	-37 ≤ h ≤ 54, -36 ≤ k ≤ 52, -50 ≤ l ≤ 23
Reflections collected	67350	37310
Independent reflections	17394 [R_{int} = 0.0651, R_{sigma} = 0.0501]	12754 [R_{int} = 0.0541, R_{sigma} = 0.0535]
Data/restraints/parameters	17394/65/847	12754/60/606
Goodness-of-fit on F^2	1.054	1.045
Final R indexes [I>=2σ (I)]	R_1 = 0.0638, $_wR_2$ = 0.1778	R_1 = 0.0936, $_wR_2$ = 0.2343
Final R indexes [all data]	R_1 = 0.0750, $_wR_2$ = 0.1872	R_1 = 0.1229, $_wR_2$ = 0.2620
Largest diff. peak/hole / e $Å^{-3}$	2.87/-3.49	1.67/-1.20

4. Bond valence sum calculations

Table S5 BVS calculation of Sn atom in **TOC-57**.

Sn1	2.093		
Sn1	Cl1	d=2.5079(19)	0.766
Sn1	Cl6	d=2.5174(18)	0.748
Sn1	O27	d=2.142(4)	0.579
Sn2	2.314		
Sn2	Cl5	d=2.415(3)	0.987
Sn2	Cl3	d=2.439(3)	0.925
Sn2	O26	d=2.277(4)	0.402
Sn3	4.085		
Sn3	Cl4	d=2.379(2)	0.759
Sn3	Cl7	d=2.3945(16)	0.726
Sn3	Cl2	d=2.3768(19)	0.759
Sn3	O5	d=2.052(4)	0.672
Sn3	O21	d=2.098(4)	0.591
Sn3	O11	d=2.109(5)	0.578

Table S6 BVS calculation of Sn atom in **TOC-58**.

Sn6	4.151		
Sn6	Cl9	d=2.415(5)	0.687
Sn6	Cl10	d=2.384(6)	0.747
Sn6	Cl12	d=2.382(6)	0.749
Sn6	O71	d=2.040(15)	0.696
Sn6	O76	d=2.068(15)	0.644
Sn6	O80	d=2.077(15)	0.628
Sn8	2.161		
Sn8	O441	d=2.315(12)	0.364
Sn8	O481	d=2.334(14)	0.344
Sn8	O56	d=2.320(13)	0.357

Sn8	O63	d=2.212(13)	0.478
Sn8	O67	d=2.118(14)	0.618

5. Additional structural pictures

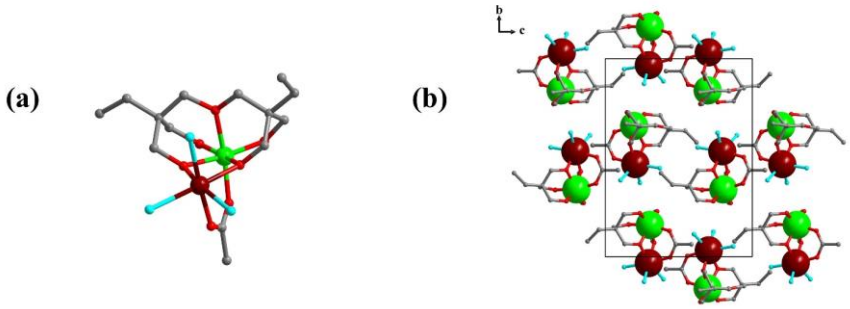

Figure S1 The cluster structure (a), and packing mode (b) of **TOC-53**. Color codes: dark red Sn; green Ti; blue Cl; gray C; red O. H atoms are omitted for clarity.

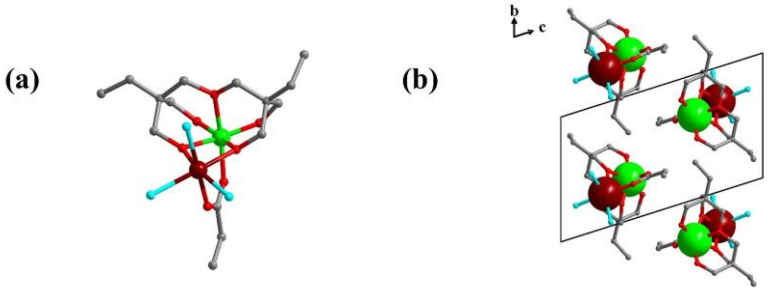

Figure S2 The cluster structure (a), and packing mode (b) of **TOC-54**. Color codes: dark red Sn; green Ti; blue Cl; gray C; red O. H atoms are omitted for clarity.

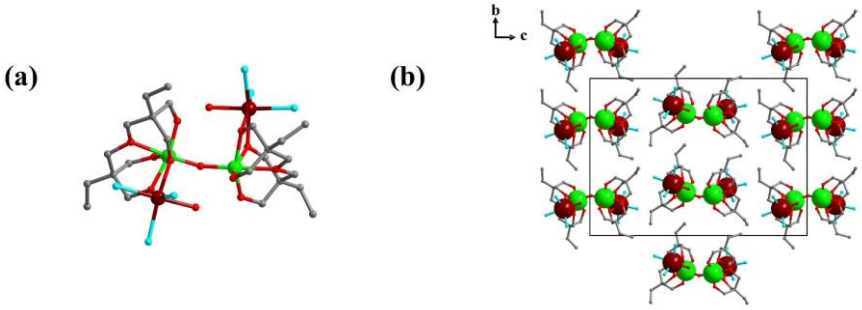

Figure S3 The cluster structure (a), and packing mode (b) of **TOC-55**. Color codes: dark red Sn; green Ti; blue Cl; gray C; red O. H atoms are omitted for clarity.

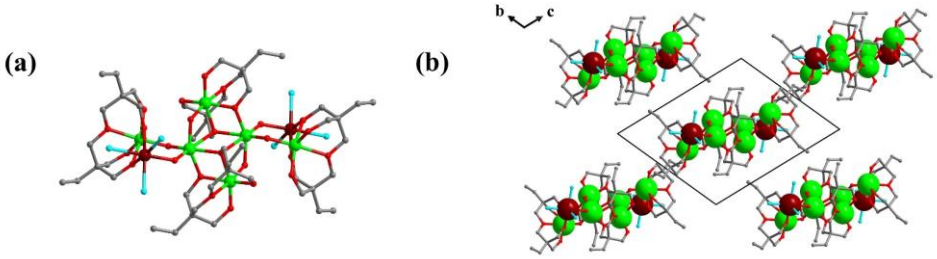

Figure S4 The cluster structure (a), and packing mode (b) of **TOC-56**. Color codes: dark red Sn; green Ti; blue Cl; gray C; red O. H atoms are omitted for clarity.

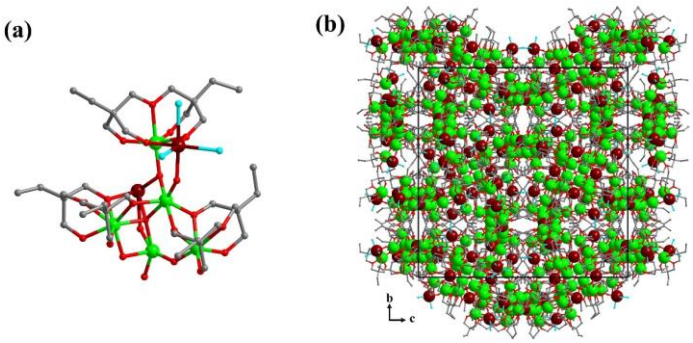

Figure S5 The asymmetric unit (a) and packing mode (b) of **TOC-58**. Color codes: dark red Sn; green Ti; blue Cl; gray C; red O. H atoms are omitted for clarity.

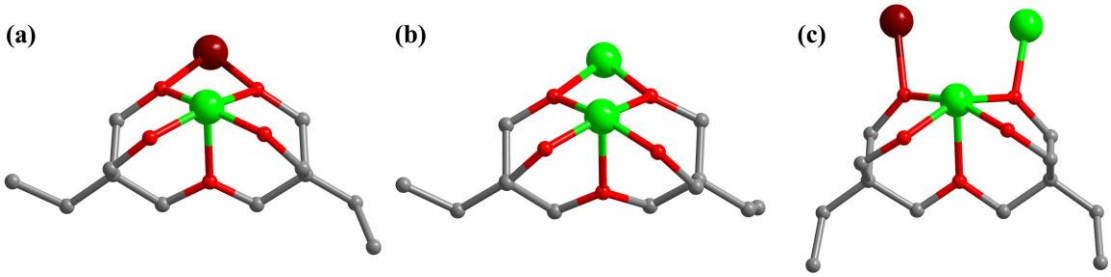

Figure S6 The chelation modes of di(trimethylolpropane) in **TOC-58.**

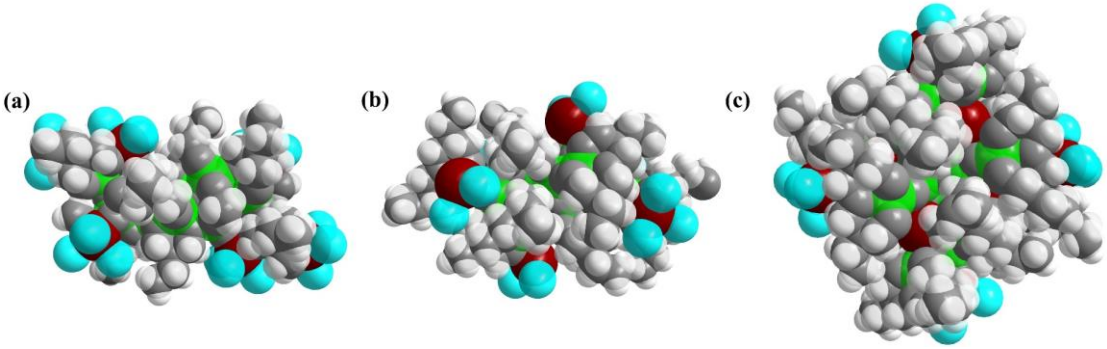

Figure S7 Space-filling model of the structures of **TOC-51** (a), **TOC-57** (b) and **TOC-58** (c), highlighting the exposed Sn atoms active sites; Color codes: dark red Sn; green Ti; blue Cl ; gray C and O ; white H.

6. Powder-XRD patterns

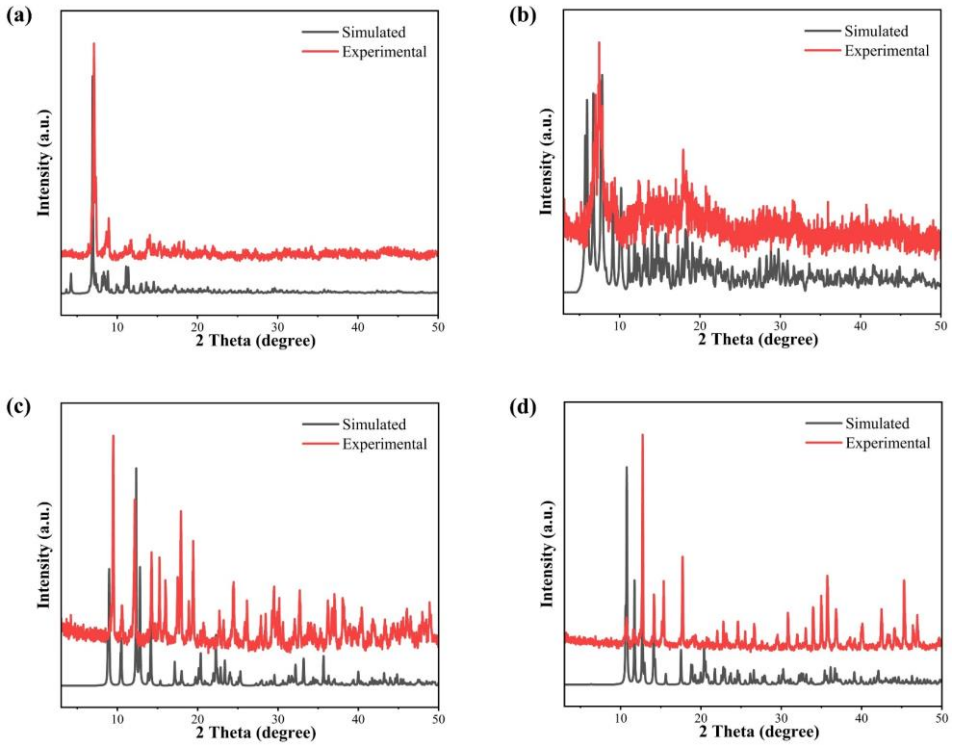

Figure S8 Simulated and experimental PXRD patterns of **TOC-51** (a), **TOC-52** (b), **TOC-53** (c) and **TOC-54** (d).

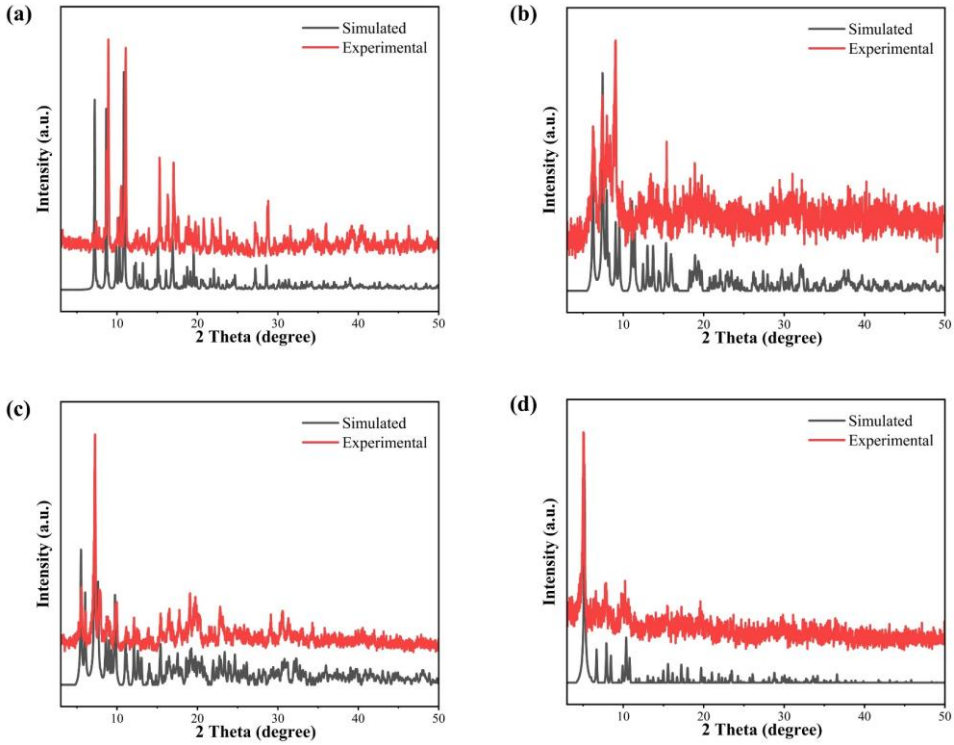

Figure S9 Simulated and experimental PXRD patterns of **TOC-55** (a), **TOC-56** (b), **TOC-57** (c) and **TOC-58** (d).

7. The energy dispersive X-ray spectroscopy (EDS) spectra

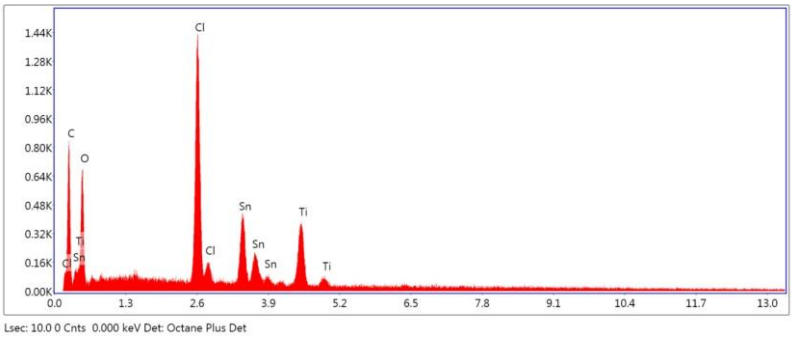

Figure S10 The EDS spectrum of **TOC-51**.

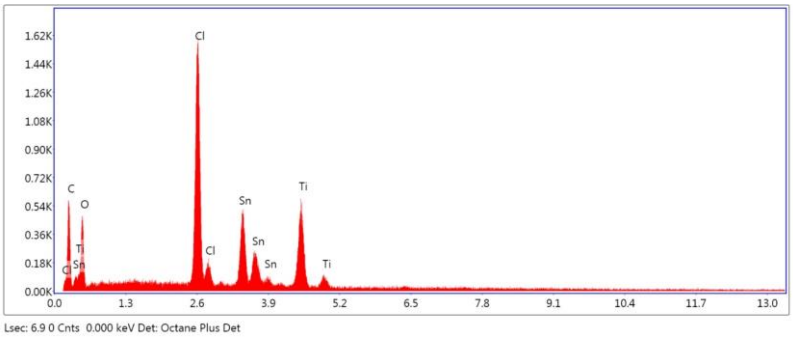

Figure S11 The EDS spectrum of **TOC-52**.

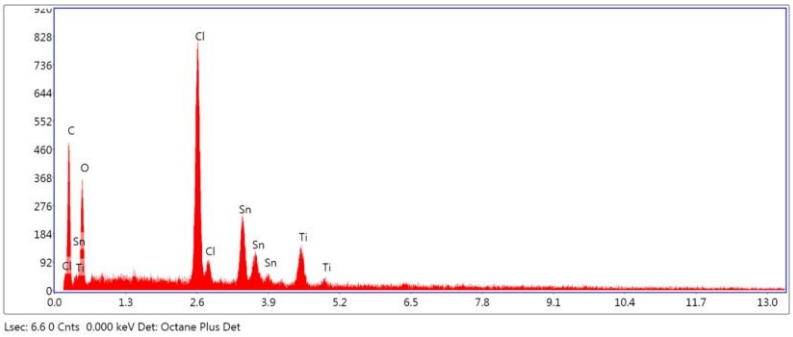

Figure S12 The EDS spectrum of **TOC-53**.

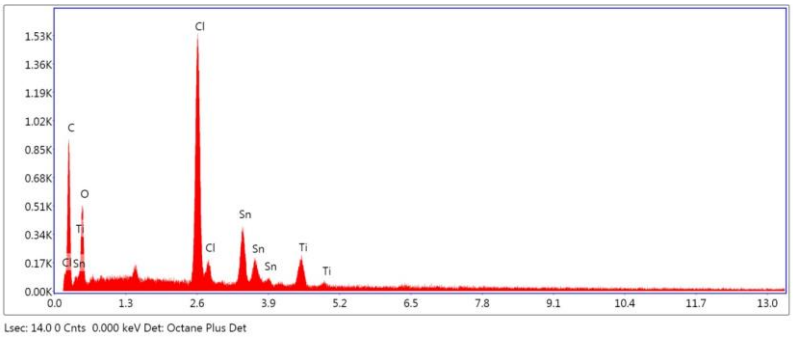

Figure S13 The EDS spectrum of **TOC-54**.

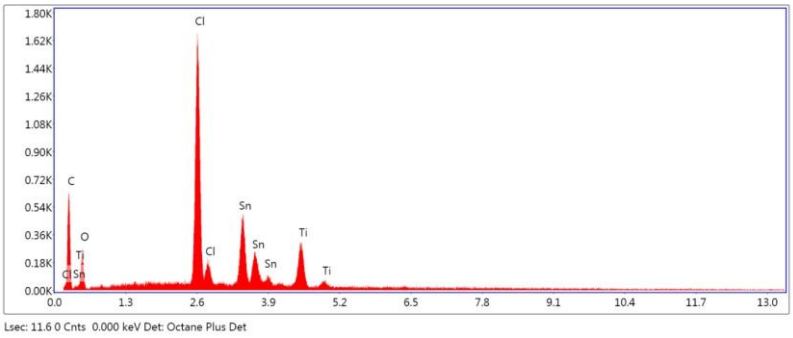

Figure S14 The EDS spectrum of **TOC-55**.

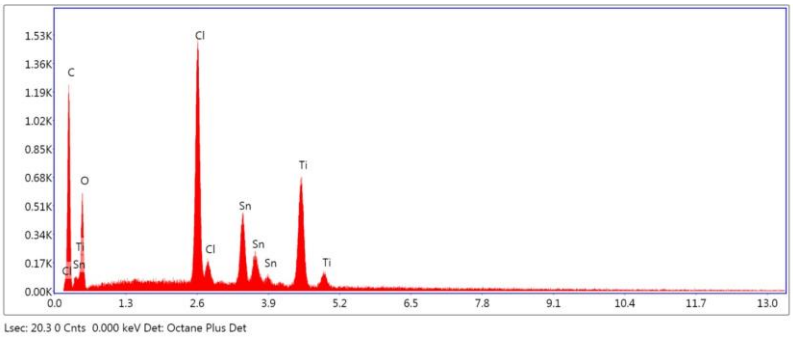

Figure S15 The EDS spectrum of **TOC-56**.

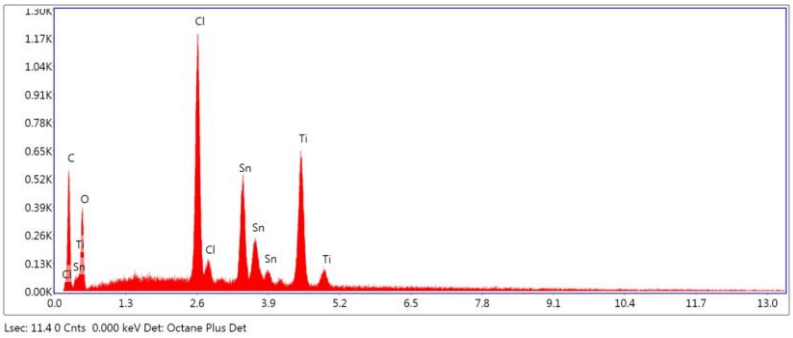

Figure S16 The EDS spectrum of **TOC-57**.

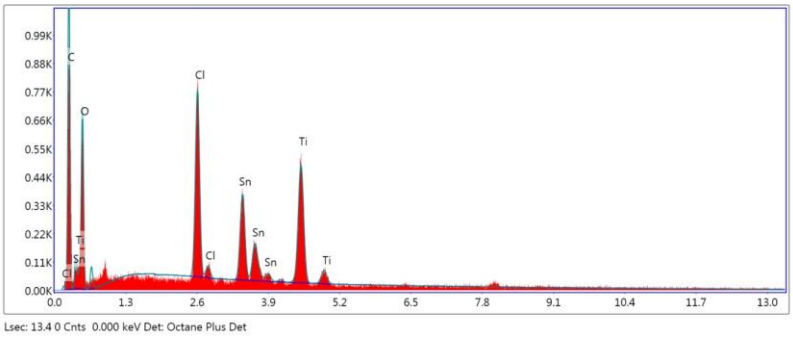

Figure S17 The EDS spectrum of **TOC-58**.

8. Thermogravimetrical analysis (TG)

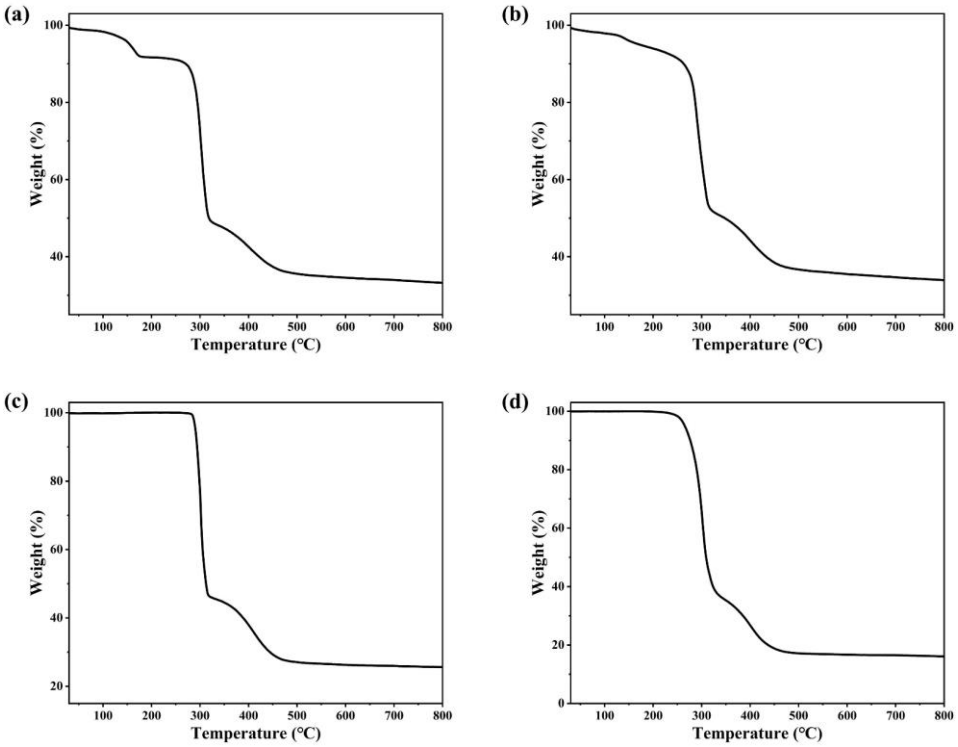

Figure S18 TG curve of **TOC-51** (a), **TOC-52** (b), **TOC-53** (c) and **TOC-54** (d) in N_2 atmosphere.

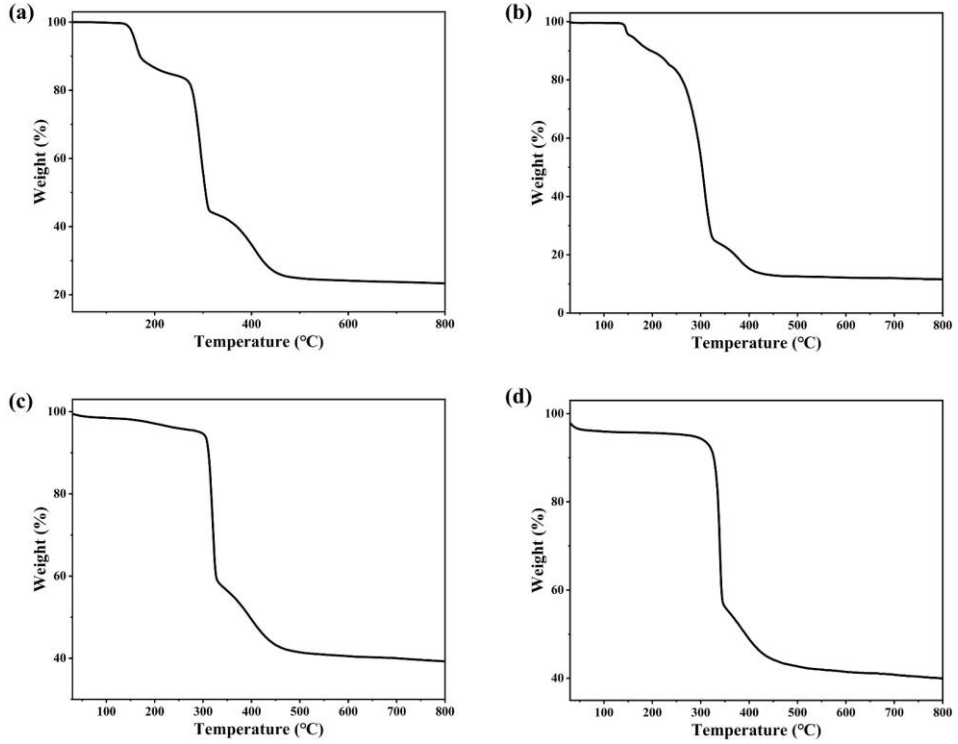

Figure S19 TG curve of **TOC-55** (a), **TOC-56** (b), **TOC-57** (c) and **TOC-58** (d) in N_2 atmosphere.

9. IR spectra

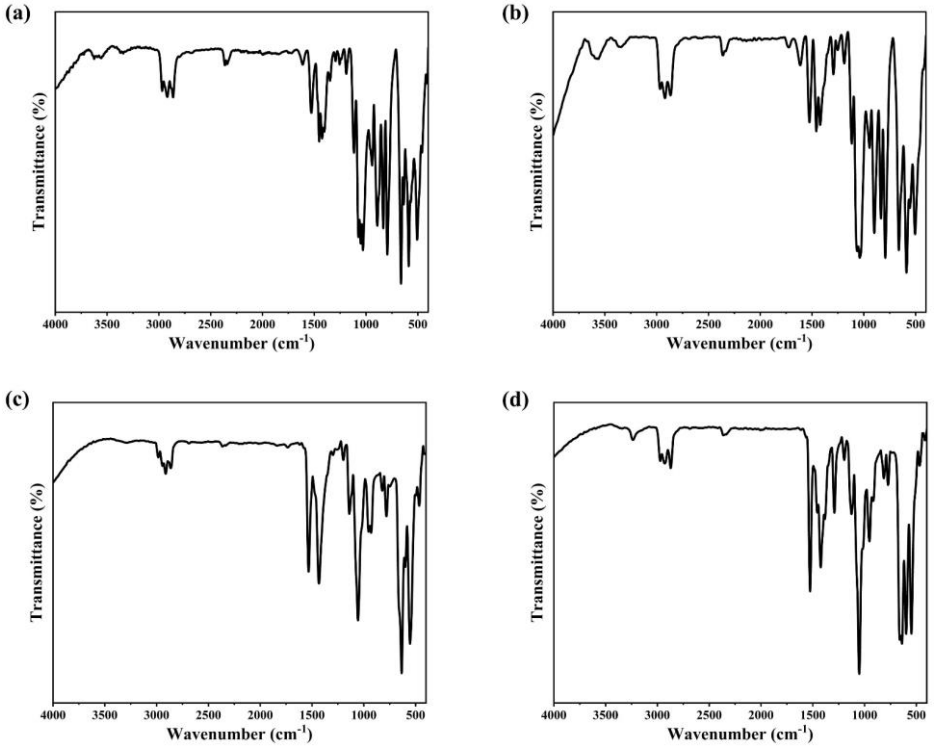

Figure S20 FT-IR spectrum of **TOC-51** (a), **TOC-52** (b), **TOC-53** (c) and **TOC-54** (d).

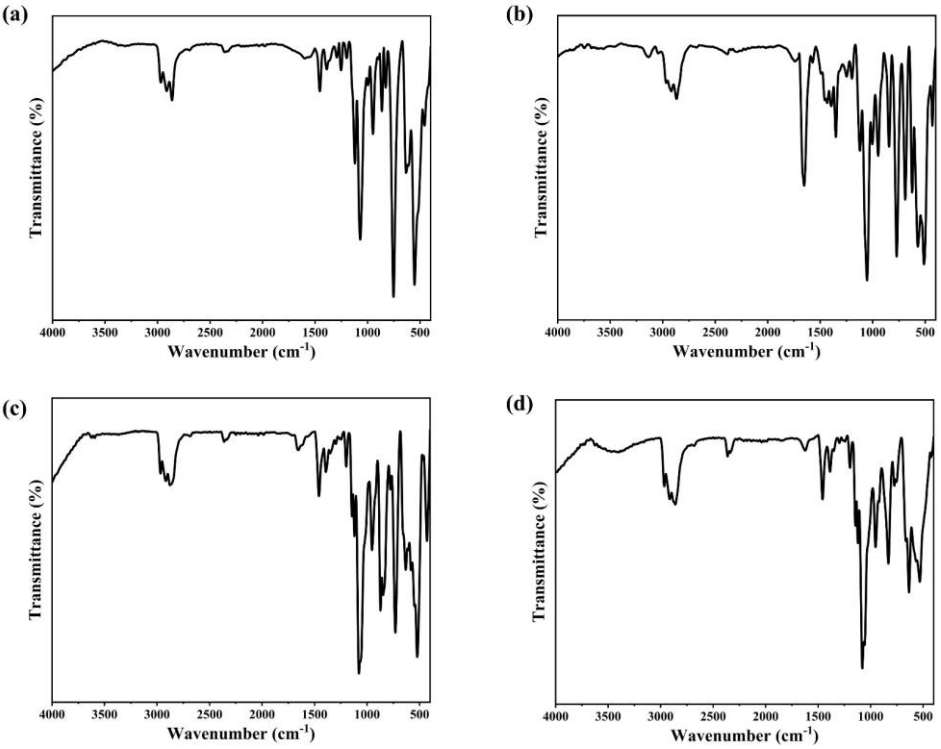

Figure S21 FT-IR spectrum of **TOC-55** (a), **TOC-56** (b), **TOC-57** (c) and **TOC-58** (d).

10. UV-Vis parameters

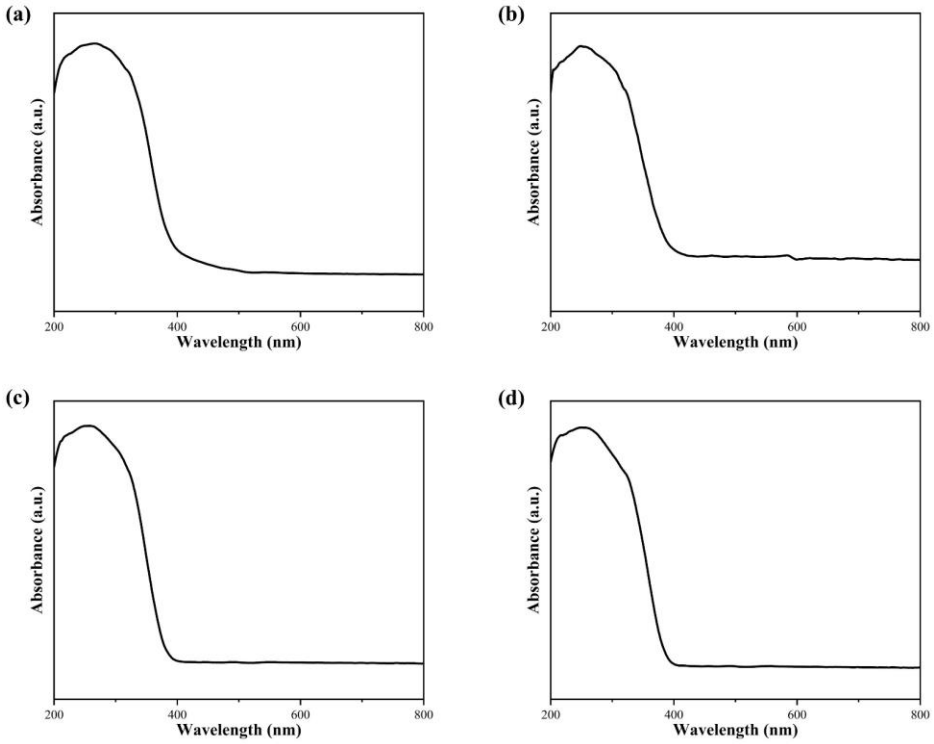

Figure S22 UV-vis diffuse reflectance spectrum of **TOC-51** (a), **TOC-52** (b), **TOC-53** (c) and **TOC-54** (d).

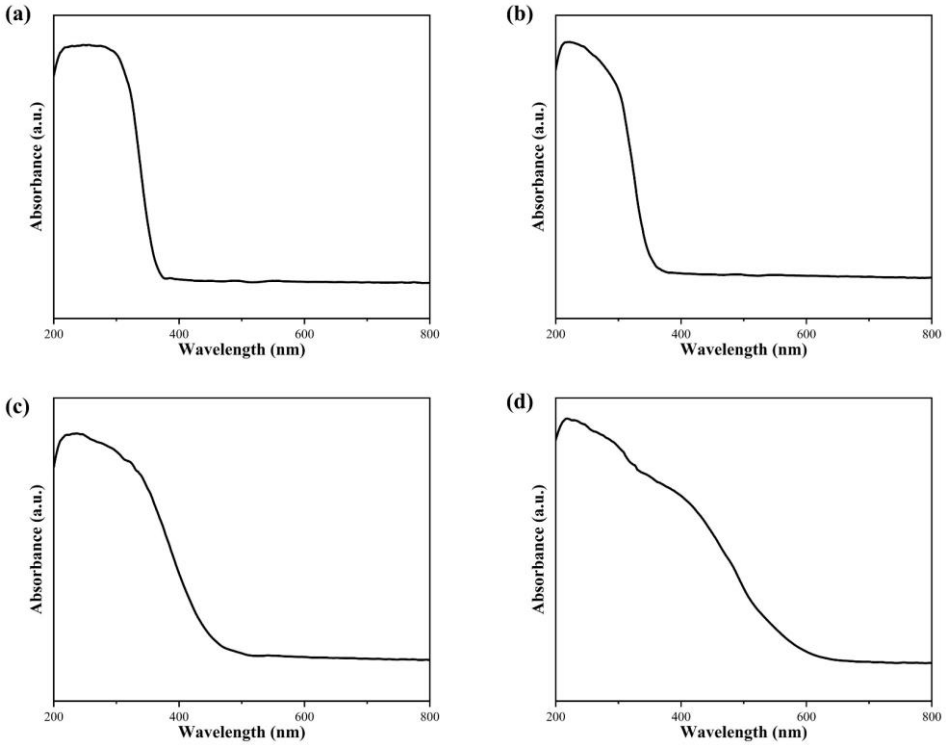

Figure S23 UV-vis diffuse reflectance spectrum of **TOC-55** (a), **TOC-56** (b), **TOC-57** (c) and **TOC-58** (d).

11. ICP results

Table S7 The summary of ICP results

Compound	Found Sn (%)	Found Ti (%)	Found	Calculated
TOC-51	18.45	12.46	Sn : Ti = 6 : 10.05	Sn : Ti = 6 : 10
TOC-52	15.28	10.86	Sn : Ti = 6 : 10.57	Sn : Ti = 6 : 10
TOC-53	16.25	8.28	Sn : Ti = 1 : 1.26	Sn : Ti = 1 : 1
TOC-54	17.37	7.13	Sn : Ti = 1 : 1.02	Sn : Ti = 1 : 1
TOC-55	15.72	7.79	Sn : Ti = 2 : 2.46	Sn : Ti = 2 : 2
TOC-56	11.11	14.32	Sn : Ti = 2 : 6.39	Sn : Ti = 2 : 6
TOC-57	17.56	16.07	Sn : Ti = 6 : 13.62	Sn : Ti = 6 : 14
TOC-58	14.91	14.91	Sn : Ti = 8 : 20.09	Sn : Ti = 8 : 20

12. Additional texts

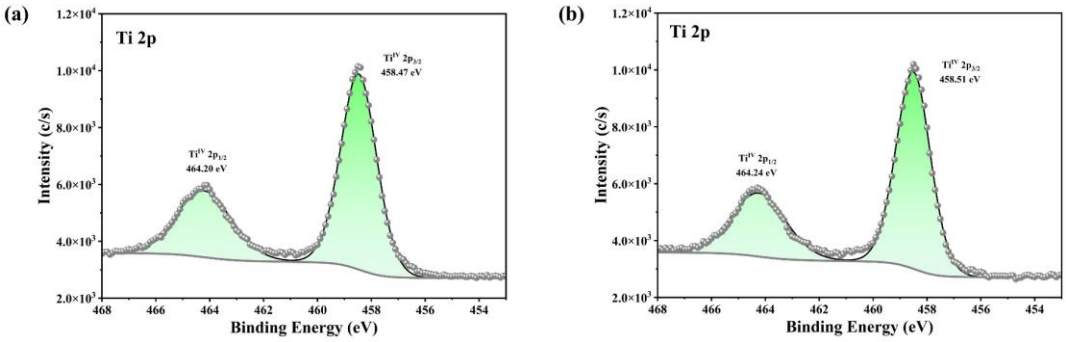

Figure S24 (a) and (b) Ti 2p XPS signals of **TOC-57** and **TOC-58**.

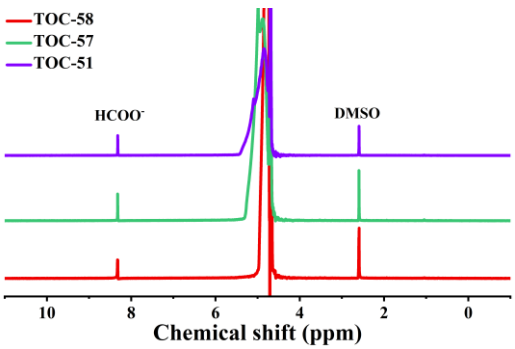

Figure S25 ^{1}H NMR spectrum of the $KHCO_3$ catholyte after 1200 s of CO_2 reduction on **TOC-51**, **TOC-57** and **TOC-58** derived electrodes, E(RHE) = −1.0 V.

13. Electrochemical Measurements

Electrochemical experiments were performed on a CHI 760e electrochemical workstation (Chenhua, Shanghai, China) using a gas-tight two-compartment electrochemical cell with a Nafion-117 proton exchange membrane as the separator. Each compartment contained 20 mL of 0.5 M $KHCO_3$ electrolyte, and the electrolyte was pre-saturated with high-purity N_2 or CO_2. The platinum net (1.0 ×1.0 cm^2) electrode and the Ag/AgCl electrode (the saturated KCl filling solution) were used as counter and reference electrode, respectively. The reference electrode potentials were converted to the value versus RHE by the equation: E (vs. RHE) = E (vs. Ag/AgCl) + 0.197 V + 0.0591 V × pH. The working electrode was prepared by pipetting the 50 uL of sample ink onto a carbon paper electrode (1×1 cm^2) with a loading of 0.53 mg/cm^2. Typically, 5.3 mg of sample was dispersed into H_2O/ethanol (370/80 uL) solution followed by adding 50 uL Nafion, then the mixture was ultrasonicated for 30 min to achieve a homogeneous ink.

For CO_2 electroreduction reaction, a flow of 20 sccm of CO_2 was continuously bubbled into the electrolyte to maintain its saturation. The linear sweep voltammetry (LSV) was performed at a scan rate of 5 mV/s. The electrolysis was conducted at selected potentials for 2 h to determine the reduction products and their Faradaic efficiencies.

Analysis of liquid products by NMR: 10.0 mL of D_2O was mixed with 3.53 μL of dimethyl sulfoxide (DMSO) as solution A for next step. Then, 500 μL of the electrolyte after electrolysis was mixed with 100 μL of D_2O and 50 μL of solution A (DMSO as internal standard) for ^1H NMR analysis. The water suppression method was used.

The gaseous products (H_2 and CO) were periodically sampled and examined by gas chromatography (GC-2014C, SHIMADZU) with N_2 as the carrier gas. They were first analyzed by a thermal conductivity detector (TCD) for the H_2 concentration, and then analyzed by flame ionization detector (FID) with a methanizer for CO. The concentration of gaseous products was quantified by the integral area ratio of the reduction products to standards.

The faradic efficiency of formate was calculated as follow [5]:

$$\mathrm{FE}(\%) = \frac{\mathrm{Q_{formate}}}{\mathrm{Q_{total}}} = \frac{n_{\mathrm{formate}} \times N \times F \times 100\%}{j \times t} \qquad (1)$$

Where $n_{formate}$ is the measured amount of formate in the cathodic compartment; N is the number of electrons required to form a molecule of formate (N = 2); F is the Faraday constant; j is the recorded current; t is the reaction time.

The faradic efficiencies of gaseous products were calculated as follow [6]:

The volume of the sample loop (V_0) in GC is 1 cm^3 and the flow rate of the gas is v = 20 cm^3/ min.

The time it takes to fill the sample loop is:

$$t_0 = \frac{V_0}{v} = \frac{1cm^3}{20cm^3/min} = 0.05min = 3s \qquad (2)$$

According to the ideal gas law, under ambient temperature of 25°C, the amount of gas in each vial (V_0 = 1 cm^3) is:

$$n = \frac{P \times V_0}{R \times T_0} = \frac{1.013 \times 10^5 Pa \times 1 \times 10^{-6} m^3}{8.314 J \cdot K^{-1} \cdot mol^{-1} \times 298.15K} = 4.0866 \times 10^{-5} mol \qquad (3)$$

The number of electrons required to form a molecule of CO or H_2 are 2. Therefore, the number of electrons (*ni*) needed to get *xi* ppm of CO or H_2 is:

$$n_i = x_i \times n \times N_A \times 2 \qquad (4)$$

Total number of electrons (n_{total}) measured during this sampling period:

$$n_{\text{total}} = \frac{j \times t_0}{e} \qquad (5)$$

The Faraday constant *F* is:

$$F = N_A \times e = 6.022 \times 10^{23} mol^{-1} \times 1.6022 \times 10^{-19} \text{C} = 96484.484 \text{C} \cdot mol^{-1} \qquad (6)$$

Hence, the faradic efficiency of CO or H_2 is:

$$\text{FE}(\%) = \frac{n_i}{n_{\text{total}}} \times 100\% = \frac{x_i \times n \times F \times 2}{I_0 \times t_0} \times 100\% \qquad (7)$$

Where *i* represents CO or H_2; I_0 is the recorded current obtained from the chronoamperogram; N_A is the Avogadro constant; *e* is elementary charge.

14. Faraday efficiency patterns

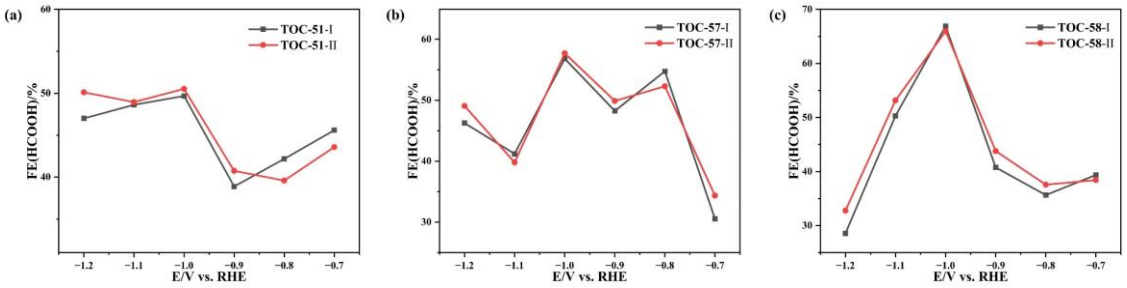

Figure S26 Comparison of formate Faraday efficiency in two electrocatalysis experiments using **TOC-51** (a), **TOC-57** (b) and **TOC-58** (c).

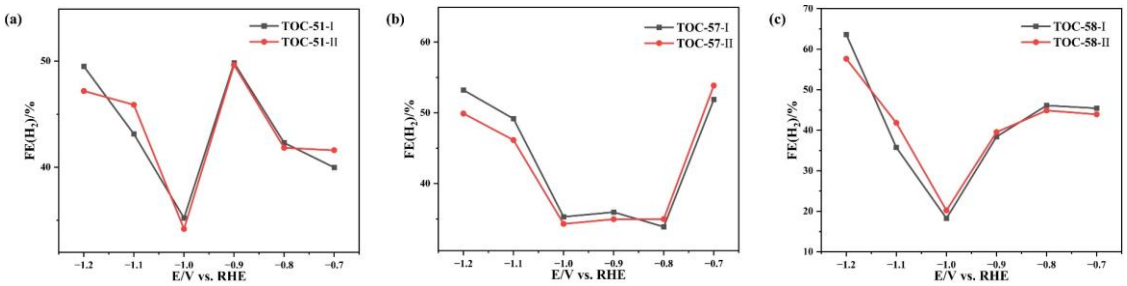

Figure S27 Comparison of H_2 Faraday efficiency in two electrocatalysis experiments using **TOC-51** (a), **TOC-57** (b) and **TOC-58** (c).

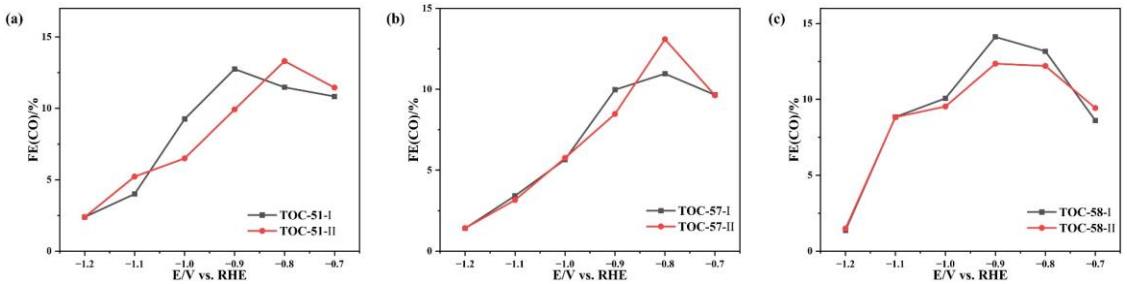

Figure S28 Comparison of CO Faraday efficiency in two electrocatalysis experiments using **TOC-51** (a), **TOC-57** (b) and **TOC-58** (c).

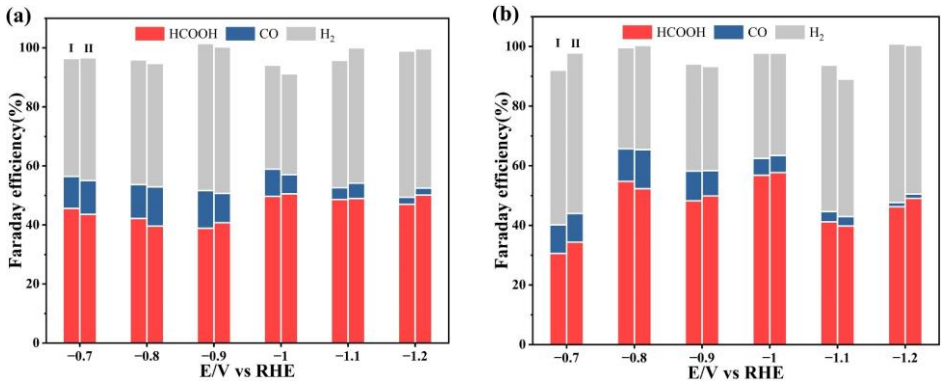

Figure S29 Faradaic efficiency of **I** (first experienment) and **II** (second experienment) at different potentials of **TOC-51** (a) and **TOC-57** (b).

15. Stability testing of compounds

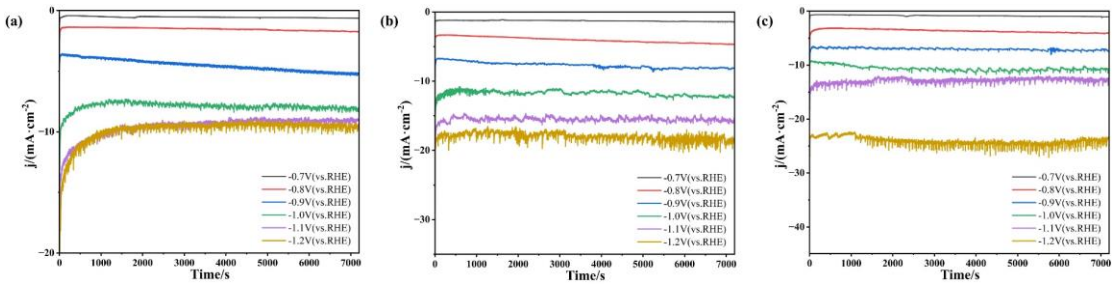

Figure S30 Total current density *vs.* time curve during electrolysis at different applied potentials of **TOC-51** (a), **TOC-57** (b) and **TOC-58** (c).

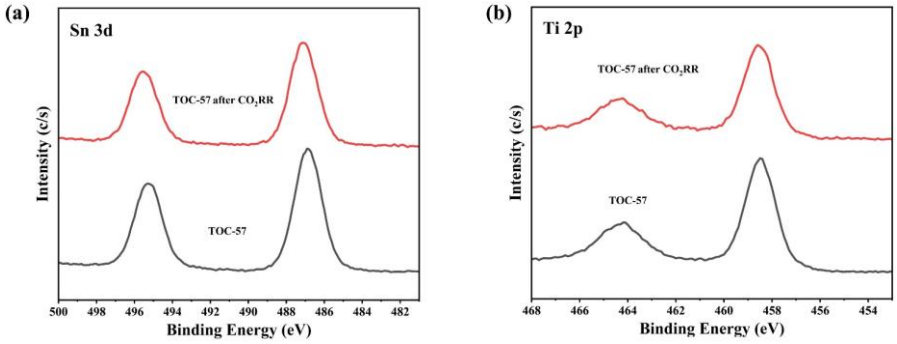

Figure S31 XPS spectrum of compound **TOC-57** before and after CO_2RR.

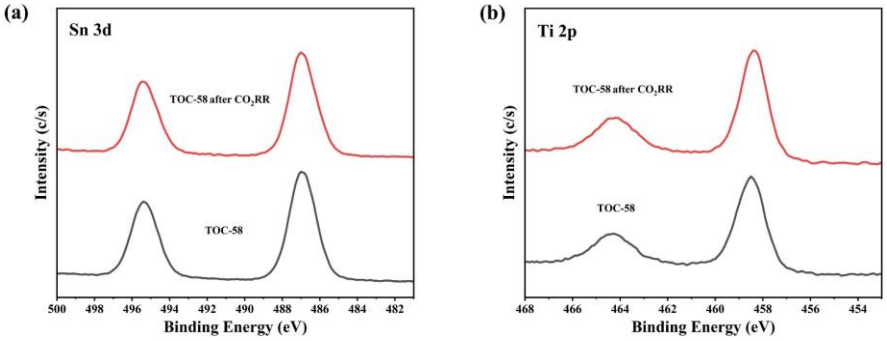

Figure S32 XPS spectrum of compound **TOC-58** before and after CO_2RR.

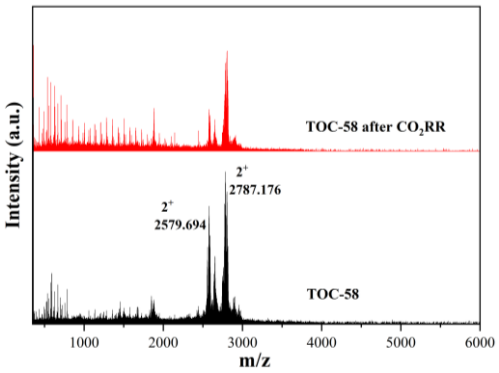

Figure S33 ESI-MS spectrum of compound **TOC-58** before and after CO_2RR.

16. Rerference

[1] O. V. Dolomanov, L. J. Bourhis, R. J. Gildea, J. A. K. Howard and H. Puschmann, OLEX2: a complete structure solution, refinement and analysis program. J. Appl. Crystallogr., 2009, 42, 339-341.

[2] G. M. Sheldrick, A short history of SHELX. Acta Crystallogr., 2008, A64, 112-22.

[3] G. M. Sheldrick, Crystal structure refinement with SHELXL. Acta Crystallogr., 2015, C71, 3-8.

[4] CrysAlisPro, Version 1.171.38.43b (Rigaku Oxford Diffraction, 2015) and CrysAlisPro 1.171.39.46 (Rigaku Oxford Diffraction, 2018) CrysAlisPro, Version 1.171.36.21 (release 14-08-2012 CrysAlis171.NET), Agilent Technologies.

[5] A.L. Spek, Acta Cryst., 2015, 71, 9-18.

[6] D. Ren, Y. Deng, A.D. Handoko, C.S. Chen, S. Malkhandi and B.S. Yeo, ACS Catal., 2015, 5, 28142821.